HHS Public Access

Author manuscript

IEEE Electron Device Lett. Author manuscript; available in PMC 2022 January 01.

Published in final edited form as:

IEEE Electron Device Lett. 2021 January ; 42(1): 46–49. doi:10.1109/led.2020.3042310.

A sub-1V, microwatt power-consumption iontronic pressure sensor based on organic electrochemical transistors

Xiaochen Wang[#],
California NanoSystems Institute, University of California-Los Angeles, Los Angeles, USA; College of Mechanical Engineering, Zhejiang University of Technology, Hangzhou, 310000, China.

Xiang Meng[#],
California NanoSystems Institute, University of California-Los Angeles, Los Angeles, USA

Yangzhi Zhu,
Terasaki Institute for Biomedical Innovation

Haonan Ling,
California NanoSystems Institute, University of California-Los Angeles, Los Angeles, USA

Yihang Chen,
California NanoSystems Institute, University of California-Los Angeles, Los Angeles, USA

Zhikang Li,
California NanoSystems Institute, University of California-Los Angeles, Los Angeles, USA; School of Mechanical Engineering, Xi'an Jiaotong University, Xi'an, 710049, China.

Martin C. Hartel,
California NanoSystems Institute, University of California-Los Angeles, Los Angeles, USA

Mehmet R. Dokmeci [Member, IEEE],
Terasaki Institute for Biomedical Innovation

Shiming Zhang [Member, IEEE],
California NanoSystems Institute, University of California-Los Angeles, Los Angeles, USA; Department of Electrical and Electronic Engineering, The University of Hong Kong, Hong Kong, China; Terasaki Institute for Biomedical Innovation

Ali Khademhosseini [Senior Member, IEEE]
California NanoSystems Institute, University of California-Los Angeles, Los Angeles, USA; Terasaki Institute for Biomedical Innovation

[#] These authors contributed equally to this work.

Abstract

Wearable and implantable pressure sensors are in great demand for personalized health monitoring. Pressure sensors with low operation voltage and low power-consumption are desired for energy-saving devices. Organic iontronic devices, such as organic electrochemical transistors

Corresponding author: S Zhang, szhang@eee.hku.hk; A Khademhosseini, khademh@terasaki.org.

(OECTs), have demonstrated great potential for low power-consumption bioelectronic sensing applications. The ability to conduct both electrons and ions, in addition to their low-operation voltage has enabled the widespread use of OECTs in different biosensing fields. However, despite these merits, OECTs have not been demonstrated for pressure sensing applications. This is because most OECTs are gated with aqueous electrolyte, which fails to respond to external pressure. Here, a low power-consumption iontronic pressure sensor is presented based on an OECT, in which an ionic hydrogel is used as a solid gating medium. The resultant iontronic device operated at voltages less than 1 V, with a power-consumption between ~ 10^1-10^3 μW, while maintaining a tunable sensitivity between 1 ~ 10 kPa^{-1}. This work places OECTs on the frontline for developing low power-consumption iontronic pressure sensors and for biosensing applications.

Keywords

Iontronic pressure sensor; OECT; hydrogel

I. Introduction

WEARABLE and implantable biosensors have gained increased attention throughout the past decade due to their potential applications in personalized healthcare monitoring [1]-[5]. Pressure sensors are used to monitor human motion and vital health signals such as heartbeat or muscle actuation. For practical wearable sensing applications, a decrease in the operation voltage and power-consumption of pressure sensors is desired for their long-term deployment on the human body.

Iontronic devices, which conduct both electrons and ions, recently emerged as advanced bioelectronic technologies at the biotic/abiotic interface [6]-[9]. Organic electrochemical transistors (OECTs) represent a typical iontronic device, which combines the merits of electrochemistry and transistors [7], [10]-[15]. Compared to conventional solid-state organic field-effect transistors, electrolyte-gated OECTs operate at much lower voltages (<1 V) and with lower power-consumption. Besides, OECTs yield a much larger transconductance (~mS) [16], [17] due to their bulk-modulation ability. Despite these merits, OECTs have rarely been developed as pressure sensors because they are often gated with an aqueous electrolyte, making it difficult to respond to external pressures [14]. We have previously reported that an ionic hydrogel can be used as a solid gating medium to develop stretchable OECTs [18].

In this letter, we demonstrate an OECT-based iontronic pressure sensor in which a microstructured ionic hydrogel was used as the solid electrolyte. Upon applying an external pressure at the gate electrode, the microstructured hydrogel deforms and changes the capacitance at the hydrogel/gate interface, ultimately changing the number of ions that are delivered to the channel. In this way, an amplified pressure signal can be obtained by measuring the output current of the OECT. With this approach, our pressure sensor was able to detect a subtle pressure of 20 Pa. Furthermore, because OECTs operate at much lower voltages (0-1 V) due to the high capacitive nature of the electrical double layer (EDL), our sensors operated with a low power-consumption between 10-1000 μW. The low-voltage

operation (<1 V) allows the sensor to work directly in aqueous environments without causing electrolysis. Additionally, low power-consumption is favorable for increasing the operational time of the sensor and reducing the overall demand on power supplies. These two advantages make the presented OECT pressure sensor a competitive candidate for wearable and implantable biosensing applications.

II. Results and Discussion

The structure of a conventional OECT is illustrated in Fig. 1(a). Conducting polymer poly (3,4-ethylenedioxythiophene) doped with poly (styrene sulfonate) (PEDOT:PSS) was employed as the channel material. Once a positive (negative) gate voltage (V_{gs}) is applied, the cations (anions) in the electrolyte are electrostatically repulsed into the conducting polymer, along with an electrochemical dedoping process in the channel. The dedoping process decreases the conductivity of the PEDOT:PSS channel, while the doping process increases the conductivity. Therefore, in PEDOT:PSS OECTs, a small change in V_{gs} leads to a larger change in source-drain current (I_d) due to the amplification effect of the OECT. It is worth mentioning that OECTs exhibit superior transconductance ($\Delta I_d / V_{gs}$) over other kinds of transistors due to their bulk doping ability (capacitance per volume) [19].

At a fixed V_{gs}, a fraction of the V_{gs} is dropped on the gate-electrolyte interface (V_g) due to the presence of the EDL_1, and the rest is dropped on the channel (V_{sol}) due to the presence of EDL_2 (shown in Fig. 1(b)). The distribution of V_g and V_{sol} depends on the capacitance ratio of EDL_1/EDL_2 (C_G/C_{CH}). We hypothesized that by employing a microstructured solid hydrogel gating medium, the C_G/C_{CH} ratio should respond to external pressure on the gate due to the mechanical deformation (Fig. 1(c-d)). In this way, at a fixed V_{gs}, the V_{sol} (which determines the output I_d of the OECT) depends only on the pressure applied to the gate electrode (Fig. 1(e)). The microstructured hydrogel was employed at EDL_1 rather than EDL_2 to simplify fabrication by avoiding an additional alignment step with the PEDOT:PSS channel. The assembled OECT pressure sensor is shown in Fig. 1(g).

The electrical performance of the OECT iontronic pressure sensor is shown in Fig. 2. The hydrogel-gated OECT operated in a low voltage range between 0 V and 0.8 V. It showed typical transistor behavior working in depletion mode and responded to external pressure (Fig. 2(a, b)). An ON/OFF ratio of ~10^2 was recorded (V_{gs} (−0.2 V)/ V_{gs} (0.8 V), source-drain voltage (V_{ds}) = −0.6 V). A decrease in I_d was observed in both the output and transfer curves upon the application of an external pressure, while a negligible current change was observed in the reference device employing flat GelMA hydrogel as the gating medium. As shown in the output curves (Fig. 2(a)), upon applying an external pressure of 100 Pa, the I_d responded when V_{gs} scanned from −0.2 V to 0.8 V. A stepwise decrease in I_d was observed in the transfer curves (Fig. 2(b)) when the pressure was varied from 0 to 250 Pa. The OECT pressure sensors showed stable current responses to the external pressure and maintained a stable baseline under different pressure values, demonstrating its reliability (Fig. 2(c)). The pressure sensor was able to detect pressure as low as 20 Pa (V_{gs} = 0.1 V, V_{ds} = −0.6 V, Fig. 2(d)), which indicates it can be used for in vitro applications such as monitoring the pressure applied by cells.

The above results validated our hypothesis and highlighted the key contribution of this work: a microstructured hydrogel-gated solid-state OECT can serve as an iontronic pressure sensor. The pressure applied on the gate determines the C_G by changing the overlapping area (A) and distance (d) between the gate electrode and hydrogel electrolyte ($C = \varepsilon_0 \varepsilon_r A/d$, where ε_0 is the vacuum permittivity, ε_r is the relative dielectric constant of the dielectric layer between two parallel plates). This process changed the V_{sol} and finally influenced the output current (I_d).

Fig. 3 shows the sensitivity of the OECT-based pressure iontronic sensor under different pressures. The sensitivity (S) is defined as follows:

$$S = \frac{\mathrm{d}((I - I_0) / I_0)}{\mathrm{d}\, p} \tag{1}$$

where p is the applied pressure, I refers to the I_d in the presence of pressure, and I_0 refers to I_d in the absence of pressure.

The highest sensitivity of 2.1 kPa^{-1} was obtained between 0 and 250 Pa (V_{gs} = 0.7 V, V_{ds} = −0.6 V). The sensitivity of the OECT iontronic pressure sensor could be controlled by changing the V_{gs}. As shown in Fig. 3(b), a higher sensitivity was extracted when we increased the V_{gs} from 0.1 V to 0.7 V. The fact that the sensitivity is controllable by V_{gs} makes our OECT iontronic pressure sensor advantageous over other conventional two-end based pressure sensors (resistive, capacitive, and piezoelectric), whose sensitivities are fixed once the device is assembled, enabling its use in more broad application scenarios.

The OECT iontronic pressure sensor operated at a low power-consumption of ~10 and μW and a low operation voltage of <1 V, which are among the lowest values reported for organic transistors-based pressure sensors (Fig. 4(b)) [20]-[28]. Power-consumption (P) of a transistor-based pressure sensor is defined in the following formula:

$$P = V_{ds} \times I_d + V_{gs} \times I_g \tag{2}$$

The low power-consumption of the presented pressure sensor stems from the low-voltage operation ability of the OECTs due to the ultrahigh capacitance of the EDL_1. For example, in the presented OECT iontronic pressure sensor, the applied V_{ds} and V_{gs} were both below 1 V. The output I_d was between μA (V_{gs} = 0.7 V) to mA (V_{gs} = 0 V), and the gate current (I_g) was negligible (μA to nA) regardless of the V_{ds}. Therefore, a low power-consumption of ~10 μW was obtained (V_{gs} = 0.7 V, V_{ds} = −0.6 V, Fig. 4(a)). In particular, a power-consumption of 2.1 * 10^{-5} W was calculated when the device showed the highest sensitivity (V_{gs} = 0.7 V, V_{ds} = −0.6 V). The low power-consumption, low operation voltage, and high output current of the OECT pressure sensor makes it a promising candidate for durable and long-term wearable and implantable applications.

Finally, to gain insight into the stability of the OECT iontronic pressure sensor, we further carried out a cyclic performance test. The performance of the device was measured under a cyclic pressure (applied by a computer-controlled tensile tester, between 0 Pa and 200 Pa), a

stable baseline was recorded with a minor change from 2.415 E^{-3} to 2.413 E^{-3} (Fig. 4(c)). The current response maintained a stable value within 100 cycles (Fig. 4(d)). A deterioration in stability was recorded after 100 cycles (~15 min), attributable to weakened ion movement in the hydrogel due to the water loss from the hydrogel. This issue is expected to be mitigated by adding salt to the hydrogel [29] and by encapsulating the device with water-impermeable elastomers [30] or plastics [31].

III. Conclusion

In conclusion, we have demonstrated an OECT-based iontronic pressure sensor that can be used for wearable and implantable biosensing applications. The sensor was developed with a microstructured solid hydrogel as the gating medium to increase the sensitivity of the OECT to external pressure. The OECT iontronic pressure sensor worked at low voltages (0~1 V) with a low power-consumption (~10 μW). Besides, the sensitivity was tunable by changing the V_{gs}. The low operation voltage, low power-consumption, and tunable sensitivity of the OECT iontronic pressure sensor make it a competitive candidate in developing low-cost pressure sensors for wearable and implantable applications.

Acknowledgments

This work was supported by the National Institutes of Health under Grant 1R01GM126571-01

References

[1]. Gao W, Emaminejad S, Nyein HYY, Challa S, Chen K, Peck A, Fahad HM, Ota H, Shiraki H, Kiriya D, Lien DH, Brooks GA, Davis RW, and Javey A, "Fully integrated wearable sensor arrays for multiplexed in situ perspiration analysis," Nature, vol. 529, no. 7587, pp. 509–514, 1. 2016, doi: 10.1038/nature16521. [PubMed: 26819044]

[2]. Zhang S, Ling H, Chen Y, Cui Q, Ni J, Wang X, Hartel MC, Meng X, Lee K, Lee J, Sun W, Lin H, Emaminejad S, Ahadian S, Ashammakhi N, Dokmeci MR, and Khademhosseini A, "Hydrogel-Enabled Transfer-Printing of Conducting Polymer Films for Soft Organic Bioelectronics," Advanced Functional Materials, vol. 30, no. 6, pp. 1906016–1906023, 11. 2019, doi: 10.1002/adfm.201906016.

[3]. Zhang S and Cicoira F, "Flexible self-powered biosensors," Nature vol. 561, no. 50, pp. 466–467, 12. 2018, doi: 10.1002/adma.201802337. [PubMed: 30258144]

[4]. Xin C, Chen L, Li T, Zhang Z, Zhao T, Li X, and Zhang J, "Highly Sensitive Flexible Pressure Sensor by the Integration of Microstructured PDMS Film With a-IGZO TFTs," IEEE Electron Device Letters, vol. 39, no. 7, pp. 1073–1076, 5 2018, doi: 10.1109/led.2018.2839595.

[5]. Sun W, Lee J, Zhang S, Benyshek C, Dokmeci MR, and Khademhosseini A, "Engineering Precision Medicine," Advanced Science, vol. 6, no. 1, pp. 1801039–1801057, 10. 2019, doi: 10.1002/advs.201801039. [PubMed: 30643715]

[6]. Zhong C, Deng Y, Roudsari AF, Kapetanovic A, Anantram MP, and Rolandi M, "A polysaccharide bioprotonic field-effect transistor," Nature communications, vol. 2, no. 1, pp. 476–480, 9. 2011, doi: 10.1038/ncomms1489.

[7]. Zhang S, Chen Y, Liu H, Wang Z, Ling H, Wang C, Ni J, Celebi-Saltik B, Wang X, Meng X, Kim HJ, Baidya A, Ahadian S, Ashammakhi N, Dokmeci MR, Travas-Sejdic J, and Khademhosseini A, "Room-Temperature-Formed PEDOT:PSS Hydrogels Enable Injectable, Soft, and Healable Organic Bioelectronics," Advanced Materials, vol. 32, no. 1, pp. 1904752–1904758, 10. 2019, doi: 10.1002/adma.201904752.

[8]. Yang C and Suo Z, "Hydrogel ionotronics," Nature Reviews Materials, vol. 3, no. 6, pp. 125–142, 5 2018, doi: 10.1038/s41578-018-0018-7.

[9]. Jia M and Rolandi M, "Soft and Ion-Conducting Materials in Bioelectronics: From Conducting Polymers to Hydrogels," Advanced Healthcare Materials, vol. 9, no. 5, pp. 1901372–1901380, 1. 2020, doi: 10.1002/adhm.201901372.

[10]. Tarabella G, Santato C, Yang SY, Iannotta S, Malliaras GG, and Cicoira F, "Effect of the gate electrode on the response of organic electrochemical transistors," Applied Physics Letters, vol. 97, no. 12, 9. 2010, doi: 10.1063/1.3491216.

[11]. Szymanski MZ, Tu D, and Forchheimer R, "2-D Drift-Diffusion Simulation of Organic Electrochemical Transistors," IEEE Transactions on Electron Devices, vol. 64, no. 12, pp. 5114–5120, 10. 2017, doi: 10.1109/ted.2017.2757766.

[12]. Sideris P, Siskos S, and Malliaras G, "Verilog-A Modeling of Organic Electrochemical Transistors," in 2017 6th International Conference on Modern Circuits and Systems Technologies (MOCAST), 2017, pp. 1–4, doi: 10.1109/MOCAST.2017.7937645.

[13]. Zhang S, Hubis E, Girard C, Kumar P, DeFranco J, and Cicoira F, "Water stability and orthogonal patterning of flexible micro-electrochemical transistors on plastic," Journal of Materials Chemistry C vol. 4, no. 7, pp. 1382–1385, 2. 2016, doi: 10.1039/c5tc03664j.

[14]. Rivnay J, Inal S, Salleo A, Owens RM, Berggren M, and Malliaras GG, "Organic electrochemical transistors," Nature Reviews Materials, vol. 3, no. 2, pp. 17086–17099, 1. 2018, doi: 10.1038/natrevmats.2017.86.

[15]. Friedlein JT, Rivnay J, Dunlap DH, McCulloch I, Shaheen SE, McLeod RR, and Malliaras GG, "Influence of disorder on transfer characteristics of organic electrochemical transistors," Applied Physics Letters, vol. 111, no. 2, pp. 023301–023304, 7. 2017, doi: 10.1063/1.4993776.

[16]. Zhang S, Kumar P, Nouas AS, Fontaine L, Tang H, and Cicoira F, "Solvent-induced changes in PEDOT:PSS films for organic electrochemical transistors," APL Materials, vol. 3, no. 1, pp. 14911–14917, 12. 2014, doi: 10.1063/1.4905154.

[17]. Dion K, Jonathan R, Michele S, Moshe G, Pierre L, H JL, Eleni S, Thierry H, Sébastien S, R. M O, and G. G M, "High transconductance organic electrochemical transistors," Nature Communications, vol. 4, no. 1 pp. 2133–2138, 7. 2013, doi: 10.1038/ncomms3133.

[18]. Zhang S, Hubis E, Tomasello G, Soliveri G, Kumar P, and Cicoira F, "Patterning of Stretchable Organic Electrochemical Transistors," Chemistry of Materials, vol. 29, no. 7, pp. 3126–3132, 2. 2017, doi: 10.1021/acs.chemmater.7b00181.

[19]. Rivnay J, Leleux P, Ferro M, Sessolo M, and Malliaras GGJSA, "High-performance transistors for bioelectronics through tuning of channel thickness," Science Advances, vol. 1, no. 4, pp. 1400251–1400255, 5 2015, doi: 10.1126/sciadv.1400251.

[20]. Schwartz G, Tee BC, Mei J, Appleton AL, Kim DH, Wang H, and Bao Z, "Flexible polymer transistors with high pressure sensitivity for application in electronic skin and health monitoring," Nat. Commun, vol. 4, no. 1, pp. 1859–1866, 5 2013, doi: 10.1038/ncomms2832. [PubMed: 23673644]

[21]. Takao S, Tsuyoshi S, Shingo I, Yusaku K, Hiroshi K, and Takayasu S, "A large-area, flexible pressure sensor matrix with organic field-effect transistors for artificial skin applications," PNAS, vol. 101, no. 27, pp. 9966–9970, 7. 2004, doi: 10.1073/pnas.0401918101. [PubMed: 15226508]

[22]. Wang Z, Guo S, Li H, Wang B, Sun Y, Xu Z, Chen X, Wu K, Zhang X, Xing F, Li L, and Hu W, "The Semiconductor/Conductor Interface Piezoresistive Effect in an Organic Transistor for Highly Sensitive Pressure Sensors," Adv. Mater, vol. 31, no. 6, pp. 1805630–1805640, 12. 2018, doi: 10.1002/adma.201805630.

[23]. Mannsfeld SC, Tee BC, Stoltenberg RM, Chen CV, Barman S, Muir BV, Sokolov AN, Reese C, and Bao Z, "Highly sensitive flexible pressure sensors with microstructured rubber dielectric layers," Nat. Mater, vol. 9, no. 10, pp. 859–864, 10. 2010, doi: 10.1038/nmat2834. [PubMed: 20835231]

[24]. Yeo SY, Park S, Yi YJ, Kim DH, and Lim JA, "Highly Sensitive Flexible Pressure Sensors Based on Printed Organic Transistors with Centro-Apically Self-Organized Organic Semiconductor Microstructures," ACS Appl. Mater. Interfaces, vol. 9, no. 49, pp. 42996–43003, 11. 2017, doi: 10.1021/acsami.7b15960. [PubMed: 29139286]

[25]. Kaltenbrunner M, Sekitani T, Reeder J, Yokota T, Kuribara K, Tokuhara T, Drack M, Schwodiauer R, Graz I, Bauer-Gogonea S, Bauer S, and Someya T, "An ultra-lightweight design

for imperceptible plastic electronics," Nature, vol. 499, no. 7459, pp. 458–463, 7. 2013, doi: 10.1038/nature12314. [PubMed: 23887430]

[26]. Takao S, Yusaku K, Tsuyoshi S, Shingo I, Yoshiaki N, Yousuke M, Hiroshi K, and Takayasu S, "Conformable, flexible, large-area networks of pressure and thermal sensors with organic transistor active matrixes," PNAS, vol. 102, no. 35, pp. 12321–12325, 8. 2005, doi: 10.1073/pnas.0502392102. [PubMed: 16107541]

[27]. Liu Z, Yin Z, Wang J, and Zheng Q, "Polyelectrolyte Dielectrics for Flexible Low-Voltage Organic Thin-Film Transistors in Highly Sensitive Pressure Sensing," Adv. Funct. Mater, vol. 29, no. 1, pp. 1806092–1806102, 11. 2018, doi: 10.1002/adfm.201806092.

[28]. Zhang Q, Leonardi F, Pfattner R, and Mas-Torrent M, "A Solid-State Aqueous Electrolyte-Gated Field-Effect Transistor as a Low-Voltage Operation Pressure-Sensitive Platform," Adv. Mater. Interfaces, vol. 6, no. 16, pp. 1900719–1900726, 7. 2019, doi: 10.1002/admi.201900719.

[29]. Bai Y, Chen B, Xiang F, Zhou J, Wang H, and Suo Z, "Transparent hydrogel with enhanced water retention capacity by introducing highly hydratable salt," Applied Physics Letters, vol. 105, no. 15, pp. 151903–151907, 10. 2014, doi: 10.1063/1.4898189.

[30]. Kim SH, Moon J-H, Kim JH, Jeong SM, and Lee S-H, "Flexible, stretchable and implantable PDMS encapsulated cable for implantable medical device," Biomedical Engineering Letters, vol. 1, no. 3, pp. 199–203, 8. 2011, doi: 10.1007/s13534-011-0033-8.

[31]. Hsu JM, Rieth L, Normann RA, Tathireddy P, and Solzbacher F, "Encapsulation of an integrated neural interface device with Parylene C," IEEE Transactions on Biomedical Engineering, vol. 56, no. 1, pp. 23–29, 1. 2009, doi: 10.1109/TBME.2008.2002155. [PubMed: 19224715]

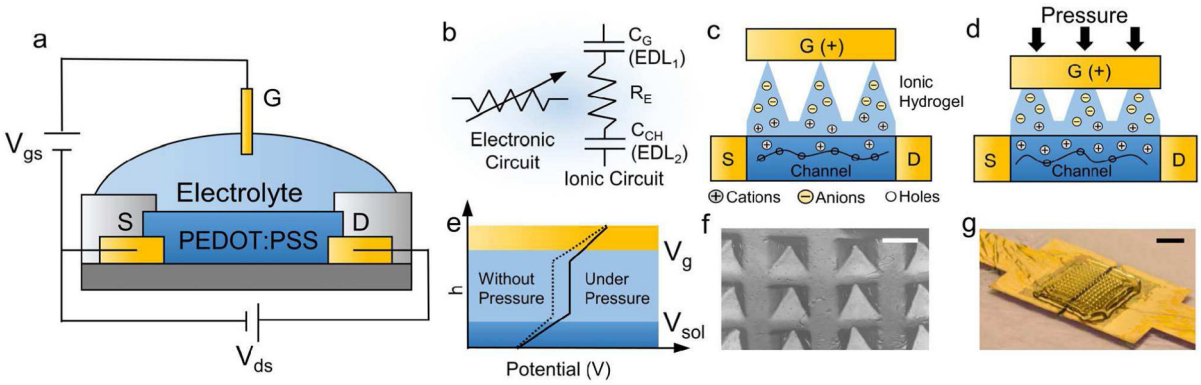

Fig. 1.

(a) Schematic diagram of the device structure of an OECT; (b) Equivalent circuits in an OECT. C_G refers to the capacitance of EDL_1 (electrolyte/gate), C_{CH} refers to capacitance of EDL_2 (electrolyte/channel), R_E refers to the resistance between gate electrolyte and channel; (c-d) Schematic diagram of the proposed microstructured hydrogel-gated OECT iontronic pressure sensor. The deformation of the hydrogel determines the number of ions delivered into the channel; (e) V_g and V_{sol} change after application of external pressure on the gate electrode; (f) Scanning electron microscopy (SEM) image of gelatin methacryloyl (GelMA) hydrogel with pyramidical microstructures on the surface, the scale bar is 1 mm. The height and base length of the pyramids are both 1 mm, and the spacing is 0.8 mm. Cetyltrimethylammonium bromide (CTAB) (0.01 M) was added into the hydrogel as the electrolyte. (g) A real optical image of the OECT iontronic pressure sensor. The scale bar is 10 mm, the channel length is 500 μm, the channel width is 20 mm, the thickness of the hydrogel is about 2 mm. The Young's modulus of the GelMA hydrogel is 15.9 kPa (water content of 80%).

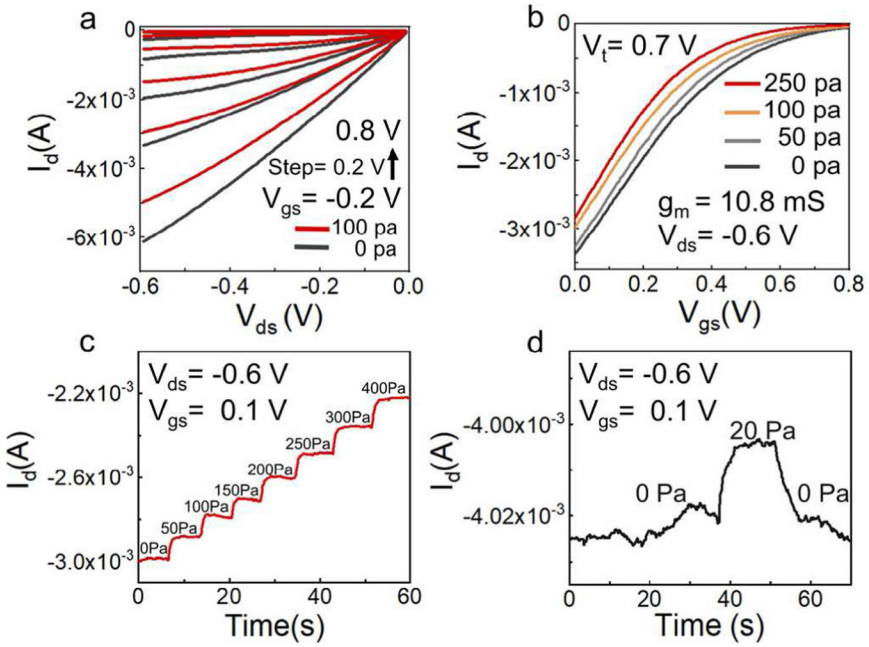

Fig. 2.

Electrical performance of an OECT iontronic pressure sensor. (a) Output curves of OECT w and w/o the application of 100 Pa pressure; (b) Transfer curves of the OECT-based pressure sensor in the presence of 0, 50, 100, 250 Pa pressure. The threshold voltage (V_t) of OECT is 0.7 V and the maximum transconductance (g_m) is calculated to be 10.8 mS (at V_{gs} = 0 V); (c) Real-time monitoring of I_d change upon a step-wise increase in pressure; (d) Real-time I_d change in the presence of 20 Pa pressure.

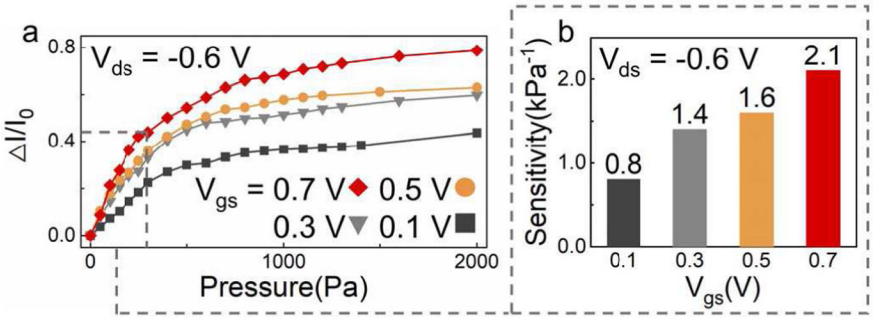

Fig. 3.

Sensitivity characterization of the OECT iontronic pressure sensor under different pressures. (a) I_d responses to pressure at different V_{gs}; (b) The pressure sensitivity (linear region) at different V_{gs}.

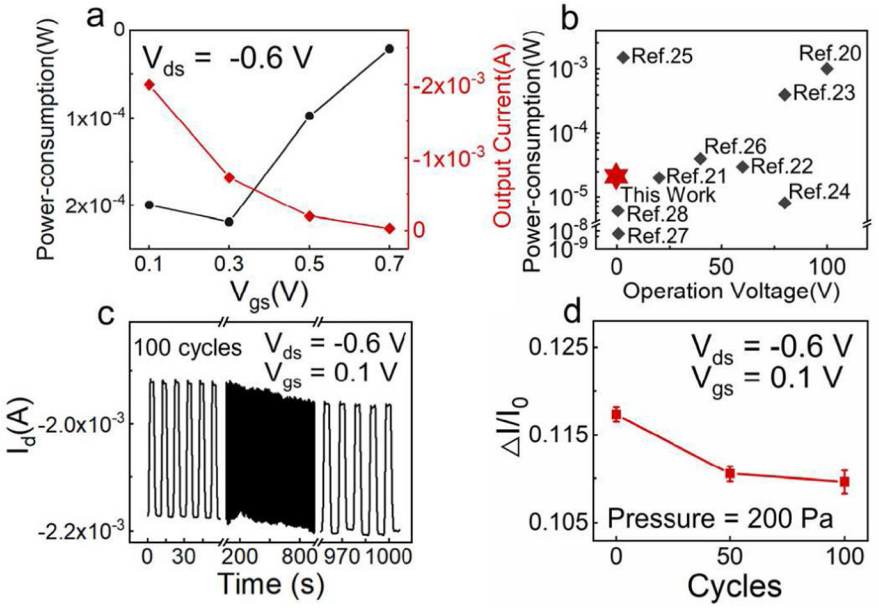

Fig. 4.

Power-consumption and stability evaluation of the OECT iontronic pressure sensor. (a) The calculated power-consumption and output I_d at different V_{gs} (pressure = 250 Pa); (b) Power-consumption and operation voltage comparison of the OECT iontronic pressure sensor with other organic transistor-based pressure sensors (the numbers correspond to the reference); (c) Stability test (I_d) of the pressure sensor for 100 cycles at the pressure of 200 Pa; (d) $\Delta I/I_0$ change within 100 pressure cycles (pressure = 200 Pa).